Electromagnetic Exposure in Greenhouse Environments under RIS-Assisted mmWave Fields

Felipe Oliveira Ribas[1,*], Günter Vermeeren[1], Thomas Zemen[2], Milica Djordjevic[2], Hamed Radpour[2], Wout Joseph[1]

[1]WAVES, Ghent University / imec, Ghent, Belgium
[2]Austrian Institute of Technology (AIT), Vienna, Austria

BioEM 2026, *Cairns, Australia*, *21-26 June 2026*

SUMMARY

The increasing use of millimeter-wave (mmWave) technologies in greenhouse environments raises questions regarding electromagnetic exposure of biological organisms, including insect pollinators and humans. While international exposure guidelines exist for humans at mmWave frequencies [1], no reference levels are available for insects, motivating quantitative exposure assessment under realistic propagation conditions.

This work models mmWave propagation using ray tracing in a realistic three-dimensional tomato greenhouse. The resulting propagation data are then used to drive full-wave FDTD exposure simulations, quantifying insect absorbed power (P_{abs}) and human absorbed power density (APD) at 26 GHz. The scene is modeled, accounting for vegetation that blocks direct paths and creates predominantly non-line-of-sight (NLoS) propagation.

Propagation scenarios include (i) an isotropic transmitter without a reconfigurable intelligent surface (RIS), (ii) a directional transmitter with a RIS, and (iii) a line-of-sight (LoS) upper-bound reference case.

Under isotropic NLoS conditions without RIS, exposure levels are extremely low, with insect P_{abs} on the order of 10^{-14}–10^{-12} W and human APD in the range of 10^{-16}–10^{-13} W/m^2. RIS-assisted directional illumination enables a stable TX–RIS–RX propagation path, restoring path gains close to the LoS reference while yielding lower exposure levels than direct LoS illumination. In this case, insect P_{abs} increases to 10^{-10}–10^{-8} W, while in the LoS reference case localized maxima approach 10^{-6} W; human APD remains in the 10^{-12}–10^{-9} W/m^2 range, several orders of magnitude below ICNIRP 2020 reference levels.

These results show that exposure is mainly governed by propagation, and that RIS-assisted systems restore connectivity while keeping exposure low.

INTRODUCTION

Smart greenhouse environments increasingly incorporate wireless sensing, automation, and monitoring systems operating at microwave and millimeter-wave frequencies (mmWave) [2]. These technologies enable high-throughput data exchange for applications such as plant monitoring, robotics, and digital-twin-based control, but also introduce new electromagnetic exposure scenarios in biologically active environments.

Greenhouses are occupied by both insect pollinators and human workers. While international exposure guidelines exist for humans at mmWave frequencies [1], no exposure limits or reference levels are defined for insects. Existing studies have investigated electromagnetic exposure of insects under free-space conditions [3], but exposure inside densely vegetated greenhouse environments—where propagation is dominated by scattering, blockage, and strong spatial inhomogeneity—has not been systematically addressed.

Reconfigurable intelligent surfaces (RISs) enable controlled reshaping of mmWave fields in obstructed environments by manipulating the phase and direction of reflected wavefronts [4]. Beyond connectivity enhancement, RISs allow exposure-aware field shaping, and recent work has shown that RIS-assisted network

planning can reduce human electromagnetic field exposure at the system level [5]. However, the implications of RIS-assisted field focusing for biologically relevant exposure metrics under realistic greenhouse propagation conditions remain largely unexplored.

In this work, RIS technology is not evaluated as a deployment or layout optimization solution. Instead, an intentionally idealized RIS configuration is used to explore conservative exposure conditions within RIS-assisted operation by maximizing coherent field focusing, and to compare them against an overall upper-bound LoS reference case. This approach allows us to assess the highest plausible exposure levels for both insects and humans under realistic greenhouse propagation constraints, providing a reference framework for future exposure-aware system design.

METHODS

Electromagnetic exposure is assessed using a two-stage simulation framework that couples deterministic propagation modeling with full-wave dosimetric analysis. Millimeter-wave propagation is simulated at 26 GHz, selected as a representative frequency within the mmWave band commonly considered for industrial and agricultural wireless systems.

Propagation setup:

A $75 \times 75 \times 10$ m tomato greenhouse containing 22 crop rows is procedurally modeled in Blender 4.5 and analyzed using the Sionna [6] ray-tracing framework (v0.19). A transmitter (TX) with an output power of 20 dBm is placed at the greenhouse entrance, and 440 receiver (RX) positions are distributed within the crop canopy in NLoS with TX to represent both potential insect and human exposure locations. Reconfigurable intelligent surface (RIS) is composed of a 30×30 element array and is placed in the center corridor in line with each row. Propagation scenarios include isotropic transmitter without RIS assistance and directional transmitters with RIS assistance (Fig. 1).

In addition to the greenhouse propagation scenarios, a line-of-sight (LoS) reference case is evaluated by placing a directional transmitter at the RIS location. This configuration removes vegetation-induced blockage and provides an upper-bound reference for achievable path gains and resulting electromagnetic exposure.

For each receiver position, the multipath components generated by Sionna are ranked by path gain, and the five strongest paths are retained. The elevation and azimuth angles, delays, and path gains of these dominant components are exported and used to define incident plane-wave excitations in subsequent finite-difference time-domain (FDTD) simulations. The receiver positions used in the ray-tracing simulations are taken as the spatial reference for the dosimetric analysis.

Exposure:

Full-wave electromagnetic simulations are performed using Sim4Life v9.0 (ZMT Zurich MedTech, Switzerland). All incident fields are simulated using unit-amplitude plane waves (1 V/m), allowing absorbed quantities to be rescaled afterward based on the ray-tracing-derived path gains to obtain realistic exposure levels.

Two exposure phantoms are considered. Insect exposure is evaluated using a photogrammetry-based model of a flying *Bombus terrestris* worker [7], represented as a homogeneous dielectric model, while human exposure is assessed using an anatomically realistic human head model from the IT'IS Foundation database [8]. For insects, total absorbed power (P_{abs}) is computed, whereas for the human model absorbed power density averaged over 4 cm^2 ($\mathrm{APD}_{4\mathrm{cm}^2}$) is evaluated, enabling comparison with established ICNIRP reference levels.

The complete workflow linking deterministic ray-tracing results to full-wave dosimetric simulations is summarized in Fig. 2.

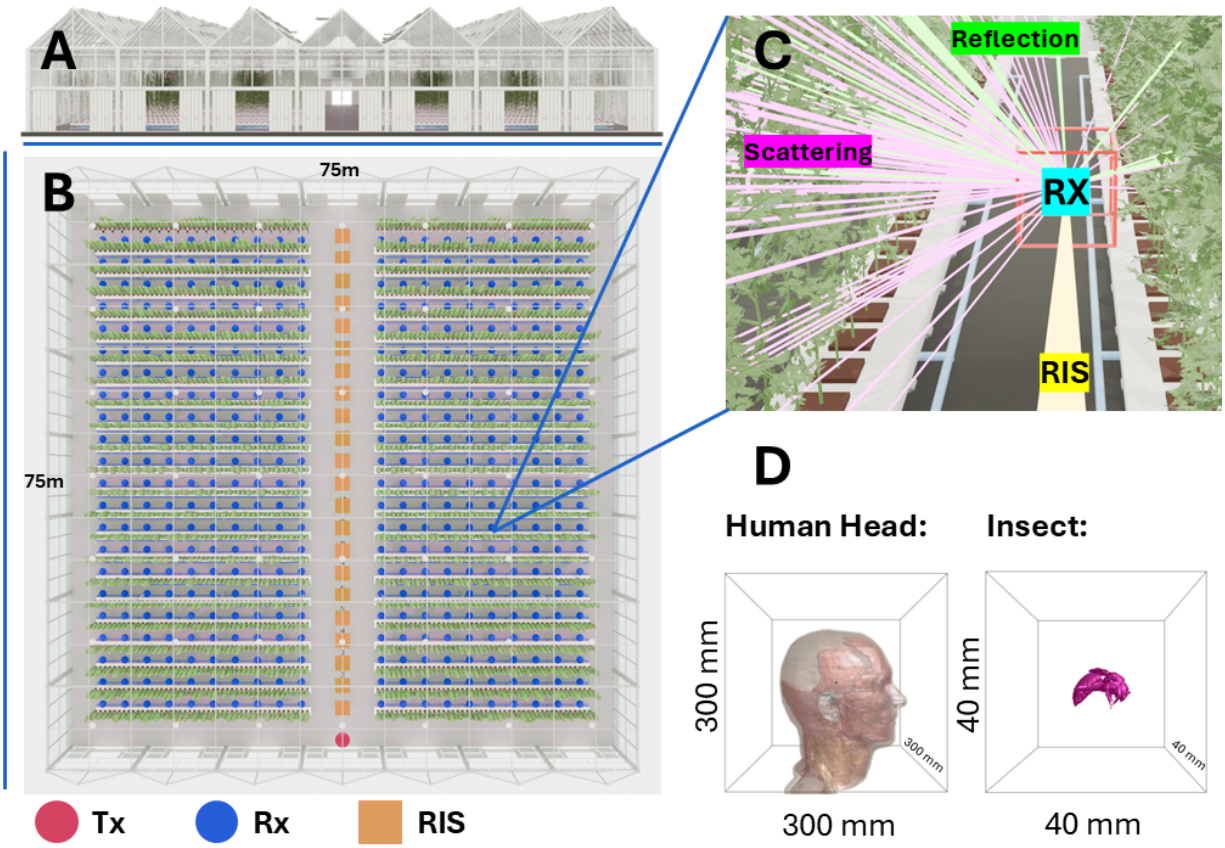

Figure 1: Overview of the simulated greenhouse environment and exposure modelling framework. (A) Side view of the tomato greenhouse structure used for ray-tracing simulations. (B) Top view of the 75×75 m greenhouse containing 22 vegetation rows separated by a central corridor. The transmitter (TX, red) is located at the corridor entrance, while receiver (RX, blue) positions are distributed as 10 RXs per row on both sides of the corridor (440 total). The reconfigurable intelligent surface (RIS), positioned along the central corridor with line-of-sight to both TX and RX rows, is shown in yellow. (C) Illustration of dominant propagation mechanisms at an RX position under RIS-assisted illumination, highlighting scattering from vegetation and controlled reflection from the RIS that forms a coherent TX–RIS–RX path. (D) Exposure phantoms used in the full-wave simulations together with their Sim4Life excitation domains: a human head model and a flying *Bombus terrestris* worker, each embedded in a cubic source region (300 mm and 40 mm side length, respectively) used to define the incident plane-wave excitation.

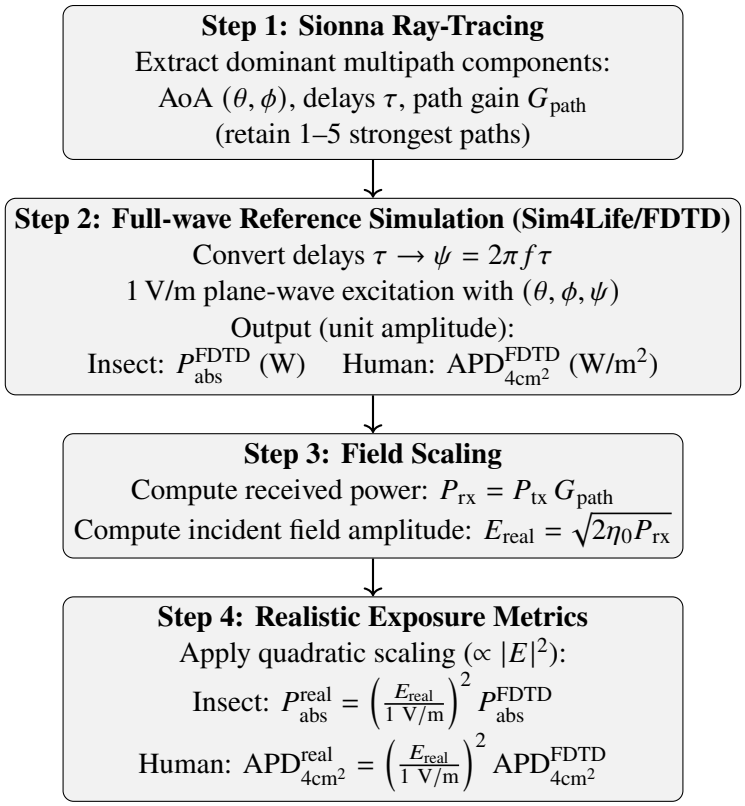

Figure 2: Workflow of the Sionna-to-Sim4Life exposure modeling pipeline for insects and humans. Ray tracing provides dominant path parameters used to define plane-wave excitations in full-wave simulations performed at unit amplitude (1 V/m). The resulting absorbed metrics (total absorbed power for insects and $\text{APD}_{4\text{cm}^2}$ for humans) are subsequently rescaled using the path-gain-derived incident field amplitude to obtain realistic exposure levels.

RESULTS

Propagation characteristics:

In the baseline scenario without RIS support, mmWave propagation inside the greenhouse is dominated by weak, incoherent scattering from dense vegetation. No line-of-sight (LoS) paths exist between transmitter and receivers, and the strongest multipath components originate from occasional reflections on metallic ceiling structures. As a result, coherent path gains are extremely low and highly variable.

When the RIS is illuminated by a directional transmitter, the dominant propagation mechanism shifts. The strongest paths consistently originate from the RIS itself, forming a deterministic TX–RIS–RX link that provides substantially higher and more stable path gains than isotropic transmission. This behavior is confirmed by the path-gain distributions, which show an increase of more than 50 dB from isotropic transmission (median ≈ -120 dB) to RIS-assisted directional illumination (median ≈ -65 dB).

As an upper-bound reference, a LoS scenario is evaluated by placing a directional transmitter directly at the RIS location. This configuration yields the highest achievable path gains, with median values around ≈ -55 dB. While the LoS case consistently exceeds the RIS-assisted scenario, the difference remains limited, indicating that RIS-assisted directional propagation can restore connectivity while remaining below the exposure levels associated with direct transmitter placement.

Insect exposure:

The propagation behavior directly translates into insect-scale exposure. In the absence of RIS support, absorbed power in the *Bombus terrestris* model remains extremely low (10^{-14}–10^{-12} W), reflecting the weak and diffuse incident fields.

When the RIS is illuminated directionally, coherent field focusing produces absorbed power levels of 10^{-10}–10^{-8} W for most receiver positions. These elevated levels are spatially confined and arise from engineered phase coherence rather than global field enhancement. In the LoS reference case, absorbed power reaches localized maxima approaching 10^{-6} W. The LoS reference scenario produces higher absorbed power than the RIS-assisted case, confirming that RIS focusing does not exceed the exposure associated with direct transmitter placement.

Human exposure:

For the human head phantom, absorption is strongly confined to superficial tissues, primarily the skin, consistent with the shallow penetration depth of mmWave fields at 26 GHz. Deeper tissues exhibit negligible absorption. This superficial absorption behavior and the use of absorbed power density (APD_{4cm^2}) as the relevant dosimetric quantity above 6 GHz are consistent with established human exposure assessment frameworks [9].

Under isotropic illumination, absorbed power density averaged over 4 cm^2 (APD_{4cm^2}) remains extremely low, with values typically in the range of 10^{-16}–10^{-13} W/m^2, reflecting the weak and incoherent incident fields inside the greenhouse. RIS-assisted directional illumination leads to a systematic increase in APD due to coherent field focusing, with most receiver positions exhibiting values between 10^{-12} and 10^{-9} W/m^2. As an upper-bound reference, the LoS scenario yields the highest absorbed power densities, reaching values on the order of 10^{-9}–10^{-8} W/m^2.

Across all simulated scenarios, APD_{4cm^2} values remain several orders of magnitude below the reference levels specified in the ICNIRP 2020 guidelines for human exposure at mmWave frequencies. Even under the conservative, high-end RIS focusing and LoS reference conditions, human exposure remains negligible from a regulatory perspective.

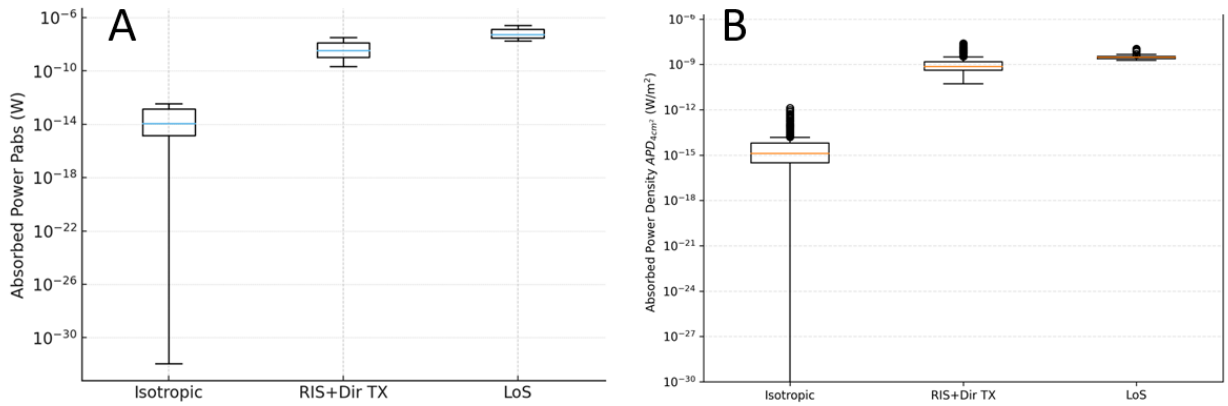

Figure 3: Comparison of electromagnetic exposure across propagation scenarios (log scale). (A) Insect exposure expressed as total absorbed power P_{abs} for a *Bombus terrestris* worker model. (B) Human exposure expressed as absorbed power density averaged over 4 cm^2 ($\text{APD}_{4\text{cm}^2}$) for an anatomically realistic human head model. Three illumination scenarios are considered: "Isotropic", representing the baseline case dominated by weak, incoherent scattered multipath; "RIS+Dir TX", corresponding to RIS-assisted directional illumination producing localized field focusing; and "LoS", denoting an upper-bound reference scenario with a directional transmitter placed at the RIS location. For insects, absorbed power is computed directly from full-wave simulations scaled by path gains. For humans, APD values simulated at unit-amplitude plane-wave excitation are rescaled using dominant propagation gains to represent realistic exposure levels. In both cases, the several-orders-of-magnitude separation between scenarios highlights the dominant role of propagation coherence and field focusing in determining exposure, rather than transmit power alone.

CONCLUSIONS

This study shows that dense vegetation in greenhouse environments operating at mmWave frequencies (26 GHz) blocks direct signal paths and creates predominantly non-line-of-sight (NLoS) propagation conditions, resulting in weak path gains and negligible exposure under isotropic operation.

RIS-assisted directional illumination enables the formation of a stable TX–RIS–RX link that raises path gains to usable levels while remaining below the upper-bound line-of-sight (LoS) reference case. Direct LoS illumination produces the highest exposure levels, with human absorbed power density reaching up to 10^{-8} W/m^2, whereas RIS-assisted illumination results in lower values, typically in the 10^{-12}–10^{-9} W/m^2 range. Across all scenarios, human exposure remains several orders of magnitude below the ICNIRP 2020 reference levels.

Insects exhibit a similar dependence on propagation conditions, with absorbed power on the order of 10^{-14}–10^{-12} W under isotropic NLoS conditions and increasing to 10^{-10}–10^{-8} W under RIS-assisted illumination, with localized maxima approaching 10^{-6} W in the LoS reference case. In the absence of established exposure guidelines for insects at mmWave frequencies, further biological studies are required to assess potential implications in agricultural environments.

REFERENCES

[1] I. C. on Non-Ionizing Radiation Protection *et al.*, "Guidelines for limiting exposure to electromagnetic fields (100 khz to 300 ghz)," *Health physics*, vol. 118, no. 5, pp. 483–524, 2020.

[2] S. Nie, M. M. Lunar, G. Bai, Y. Ge, S. Pitla, C. E. Koksal, and M. C. Vuran, "mmwave on a farm: Channel modeling for wireless agricultural networks at broadband millimeter-wave frequency," in *2022 19th Annual IEEE International Conference on Sensing, Communication, and Networking (SECON)*, pp. 388–396, IEEE, 2022.

[3] A. Thielens, D. Bell, D. B. Mortimore, M. K. Greco, L. Martens, and W. Joseph, "Exposure of insects to radio-frequency electromagnetic fields from 2 to 120 ghz," *Scientific reports*, vol. 8, no. 1, p. 3924, 2018.

[4] H. Radpour, M. Hofer, D. Löschenbrand, L. W. Mayer, A. Hofmann, M. Schiefer, and T. Zemen, "Reconfigurable intelligent surface for industrial automation: mmwave propagation measurement, simulation, and control algorithm requirements," in *2024 IEEE 35th International Symposium on Personal, Indoor and Mobile Radio Communications (PIMRC)*, pp. 1–7, IEEE, 2024.

[5] B. Yin, W. Joseph, and M. Deruyck, "Ris-aided mmwave network planning toward connectivity enhancement and minimal electromagnetic field exposure," *IEEE Access*, vol. 11, pp. 115911–115923, 2023.

[6] J. Hoydis, S. Cammerer, F. A. Aoudia, A. Vem, N. Binder, G. Marcus, and A. Keller, "Sionna: An open-source library for next-generation physical layer research," *arXiv preprint arXiv:2203.11854*, 2022.

[7] Yuichi Kano, "Cc0 bumblebee." https://sketchfab.com/3d-models/cc0-bumblebee-f0aac424f44b48cf9217ffe126ace5ca, 2020. 3D model obtained via photogrammetry. Licensed under CC0 Public Domain.

[8] IT'IS Foundation, "Ixi heads v1.0." Virtual Population — Regional Human Models, 2024. Release Date: 18 June 2024.

[9] A. Hirata, Y. Diao, T. Onishi, K. Sasaki, S. Ahn, D. Colombi, V. De Santis, I. Laakso, L. Giaccone, W. Joseph, *et al.*, "Assessment of human exposure to electromagnetic fields: Review and future directions," *IEEE Transactions on Electromagnetic Compatibility*, vol. 63, no. 5, pp. 1619–1630, 2021.